HHS Public Access

Author manuscript

Kidney Int. Author manuscript; available in PMC 2013 April 01.

Published in final edited form as:

Kidney Int. 2012 October ; 82(8): 867–877. doi:10.1038/ki.2012.223.

Overexpression of stanniocalcin-1 inhibits reactive oxygen species and renal ischemia/reperfusion injury in mice

Luping Huang, MD, PhD[1], **Tatiana Belousova, MD**[1], **Minyi Chen**[1], **Gabriel DiMattia, PhD**[2], **Dajun Liu, MD**[1,3], and **David Sheikh-Hamad, MD**[1,*]

[1]Division of Nephrology, Department of Medicine, Baylor College of Medicine, The University of Western Ontario, London, Ontario, Canada

[2]Departments of Oncology and Biochemistry, The University of Western Ontario, London, Ontario, Canada

[3]China Medical University, Sheng Jing Hospital, PR China

Abstract

Reactive oxygen species, endothelial dysfunction, inflammation, and mitogen-activated protein kinases have important roles in the pathogenesis of ischemia/reperfusion kidney injury. Stanniocalcin-1 (STC1) suppresses superoxide generation in many systems through induction of mitochondrial uncoupling proteins and blocks the cytokine-induced rise in endothelial permeability. Here we tested whether transgenic overexpression of STC1 protects from bilateral ischemia/reperfusion kidney injury. This injury in wild type mice caused a halving of the creatinine clearance; severe tubular vacuolization and cast formation; increased infiltration of macrophages and T cells; higher vascular permeability; greater production of superoxide and hydrogen peroxide; and higher ratio of activated ERK/activated JNK and p38, all compared to sham-treated controls. Mice transgenic for human STC1 expression, however, had resistance to equivalent ischemia/reperfusion injury indicated as no significant change from controls in any of these parameters. Tubular epithelial cells in transgenic mice expressed higher mitochondrial uncoupling protein 2 and lower superoxide generation. Pre-treatment of transgenic mice with paraquat, a generator of reactive oxygen species, before injury restored the susceptibility to ischemia/reperfusion kidney injury, suggesting that STC1 protects by an anti-oxidant mechanism. Thus, STC1 may be a therapeutic target for ischemia/reperfusion kidney injury.

Keywords

vascular permeability; mitochondria; free radicals; inflammation

*Corresponding author: David Sheikh-Hamad, M.D.; One Baylor Plaza; ABBR R706; M/S BCM395; Houston, TX 77030-3498; Tel: 713-798 1301; FAX: 713-798 5010; sheikh@bcm.tmc.edu.

Disclosure: no financial interest to disclose.

Introduction

Ischemic acute kidney injury (AKI) is common and leads to kidney failure quite often. An acute ischemic insult occurring immediately after kidney transplantation – contributes to "early graft dysfunction", and may lead to chronic allograft nephropathy [1;2]; while, an increase in serum creatinine in post-surgical patients is associated with poor outcomes [3;4]. Moreover, a recent study by Chertow and colleagues, suggested that a small increase in serum creatinine in patients admitted to the hospital is associated with increased mortality, longer hospitalizations and higher cost of care [5]. While we have better understanding of the pathogenesis of ischemic kidney injury, few therapeutic options are currently available.

Experimental mouse I/R kidney injury has been used extensively to study the pathogenesis of ischemic AKI. Increased generation of reactive oxygen species (ROS), endothelial dysfunction, vascular congestion at the cortico-medullary junction, and inflammation, are critical players in the pathogenesis of I/R kidney injury [6–10]. T-cells and macrophages play important roles in the injury and repair [11–14], and are believed to home-in on the injured kidney in response to inflammatory cytokines such as macrophage chemotactic protein-1 (MCP-1), and tumor necrosis factor-1α (TNF-1α), produced locally by cells such as the resident dendritic cells and injured tubular and endothelial cells [15;16]. In addition, activation of mitogen activated protein kinases (MAPKs) occurs immediately after injury [17], and high ratio of active extracellular regulated kinase (p-ERK) over active June-N-terminal kinase (p-JNK) plus active p38 kinase (p-p38) has been shown to correlate with protection from I/R kidney injury [18].

Studies from our lab show STC1 suppresses superoxide generation through induction of mitochondrial uncoupling proteins [19]. In cytokine-treated endothelial monolayer, we have shown that treatment with STC1: decreases superoxide generation and the activation of pro-inflammatory signaling pathways, JNK and Nuclear Factor-κB (NF-κB) [20]; preserves endothelial barrier function [20], and decreases transendothelial migration of inflammatory cells (T-cells and macrophages) [21]. On the other hand, treatment of macrophages with STC1, suppresses superoxide generation [22], and decreases the mobility and response of macrophages to chemoattractants [23].

Mammalian STC1 is ubiquitously expressed [24]. It is secreted as phosphoglycoprotein [25;26], and is thought to function in an autocrine/paracrine manner [27;28]. However; recent reports suggest that mammalian STC1 is also blood borne [29;30] – attached to a soluble protein [29]; and thus, may have additional hormonal functions. STC1 binds to a cell surface receptor and is targeted to the mitochondria [31]; and subcellular fractionation suggested that more than 90% of cellular STC1 immunoreactivity is mitochondrial [31]. Consistent with these data, we found that addition of recombinant STC1 protein to the medium of cultured macrophages or cardiomyocytes, is followed by sequestration of the protein in the mitochondria, upregulation of uncoupling proteins and suppression of superoxide generation [19;22]. The internalization of STC1 into the cell, targeting to- and action in the mitochondria, define STC1 as an intracrine factor [32].

Based on the above observations, we hypothesized that STC1 protects from I/R kidney injury through its effects to: decrease the generation of ROS; stabilize endothelial barrier function; and inhibit inflammation. To test this hypothesis, we applied a well established mouse I/R kidney injury model to WT and STC1 Tg mice that display in the kidney preferential expression of STC1 transgene in endothelial cells and macrophages [30], and examined a number of functional, morphological and biochemical parameters that correlate with kidney injury after I/R. Our data suggest that transgenic overexpression of STC1 confers resistance to I/R kidney injury through suppression of oxidant stress.

Results

Transgenic overexpression of STC1 confers resistance to I/R kidney injury: STC1 Tg mice display no change in kidney function or morphology after I/R

Because of the differences in weight between WT and STC1 Tg mice, we could not rely on changes in serum creatinine for the assessment of renal function after I/R; hence, to obtain reliable estimates of glomerular filtration rate, we measured CrCl and corrected it for the weight. However, this introduced a caveat. CrCl values for each time point are based on urine collections that began 20 hours earlier; i.e., urine collection for the 24h time point was started 4h after I/R or sham operation, and before the full kidney injury had occurred. Therefore, the CrCl values for the 24h time point do not reflect the full extent of renal injury in WT kidney, as revealed by the histology 24h after I/R. Following I/R and compared to sham-treated controls, WT mice displayed: 50% drop in CrCl at the 48h and 72h time points after I/R (Fig. 1); severe cellular vacuolization, tubular dilatation and cast formation, that were observed starting 24h after I/R, and persisted through the 72h time point (Fig. 2B, 2C and 2D). In contrast, STC1 Tg mice displayed no change in CrCl or kidney morphology at any time point after I/R. As previously reported [18], we observed full recovery of kidney function (Fig. 1) and morphology (Fig. 2E) in WT mice by day 8. The data suggest that Tg overexpression of STC1 confers resistance to I/R kidney injury. Of note, loss of brush border membrane is characteristic of I/R kidney injury [33;34], and the absence of such changes in the kidneys of STC1 Tg mice (Fig. 2F–2J) is consistent with resistance to I/R injury. Of interest, STC1 protein expression is induced in WT kidneys at the 24h time point following I/R, but not in STC1 Tg kidneys, and this induction occurs mostly in injured tubule cells, consistent with STC1 function as cell stress gene. Staining for STC1 in Tg kidneys remained unchanged, and was prominent in blood vessels (Fig. 3).

Increased infiltration with macrophages and T-cells in WT kidneys following I/R, but not in STC1 Tg kidneys—Inflammation plays an important role in the pathogenesis of I/R kidney injury; and while the role of neutrophils remains uncertain [35;36], T-cells and macrophages appear to be critical [11;37]. Using immunohistochemistry, we examined the kidneys for infiltration with T-cells (CD3) and macrophages (F4/80 and CD68) following I/R. Compared to sham-treated controls: WT kidneys displayed increased infiltration with T-cells (Fig. 4A) and macrophages [F4/80 shown in Fig. 4B; staining with the pan macrophage marker CD68 showed similar results; data not shown], starting 24h after I/R, and persisting through day 8. In contrast, kidneys of Tg mice displayed no change in the number of T-cells or macrophages after I/R. The data

suggest two possibilities: 1) Tg overexpression of STC1 inhibits inflammation in the kidneys following I/R; alternatively, 2) the resistance of STC1 Tg mice to I/R kidney injury obviates the inflammatory response.

Increased activities of MAPKs in the kidneys of WT mice after I/R, but not in the kidneys of STC1 Tg mice—The activities of MARKs ERK, JNK, and p38 increase markedly after ischemia *in vivo* and chemical anoxia *in vitro* [38]. The relative extent of activation of ERK, JNK, or p38 has been proposed to determine cell fate after I/R kidney injury [18;39;40]; and the post-ischemic activation patterns of MAPKs may contribute to the protection afforded by ischemic pre-conditioning, whereby a higher ratio of p-ERK/p-p38+ p-JNK promotes cell survival [18].

STC1 has been reported to attenuate ERK activity in mouse embryo fibroblasts [41], and with that in mind, we sought to determine the activities of MAPKs in the kidneys 24h, 48h, 72h and 8d following I/R utilizing two approaches: 1) immunohistochemistry, counting positively stained cells for p-MAPKs in 10 grids spanning cortico-medullary junction, where most of MAPK activation following I/R occurs; 2) similarly, Western blot analysis using lysates representing whole kidney, where p-ERK/ERK was divided by the sum of p-JNK/JNK and p-p38/p38. We found an increase in the number of tubular cells positive for p-ERK, p-JNK and p-p38 in WT kidneys after I/R; however, we observed no change in the number of cells stained positive for p-ERK, p-JNK or p-p38 in STC1 Tg kidneys (Fig. 5). Similarly, Western blot analysis revealed a significant increase in the activities of all three MAPKs, and a higher ratio of p-ERK/p-JNK+p-p38 in WT kidney lysates at the 24h time point after I/R, but not in STC1 Tg kidney lysates (Fig. 6). Since activation of MAPKs following I/R is an indication of acute injury, our data are consistent with lack of injury in STC1 Tg kidneys after I/R. In addition, one may also conclude that resistance to I/R kidney injury in STC1 Tg kidneys occurred in spite of the lower relative ratio of p-ERK/p-p38+p-JNK.

Increased vascular permeability after I/R injury in WT kidneys, but not in STC1 Tg kidneys—Excessive generation of ROS has been implicated in the pathophysiology of endothelial barrier dysfunction after I/R [7;8]. Disruption of the integrity of this barrier markedly increases permeability to fluids, macromolecules and inflammatory cells [42]. In cytokine-treated endothelial monolayer, we have shown STC1 attenuates superoxide generation [20], maintains the expression of tight junction proteins [20], stabilizes endothelial barrier function [20] and diminishes transendothelial migration of T-cells and macrophages [21]. Measuring Evans blue dye retention in the kidney as a correlate of vascular permeability *in vivo*, we found higher Evans blue retention in WT kidneys 5h after I/R, but not in STC1 Tg kidneys (Fig. 7). The data are consistent with our hypothesis that STC1 stabilizes endothelial barrier function *in vivo*, a mechanism that may contribute to/or underlie the resistance of STC1 Tg mice to I/R kidney injury.

Increased generation of superoxide and H_2O_2 after I/R in WT kidneys, but not in STC1 Tg kidneys—There is substantial evidence to support a role for ROS in the pathogenesis of AKI [43]. STC1 has been shown by us to decrease superoxide generation through induction of mitochondrial uncoupling proteins [22]. In the following experiment,

we employed semi-quantitative methods to measure superoxide and H_2O_2 in the kidneys of WT and STC1 Tg mice 24h after I/R, and found marked elevation in both superoxide and H_2O_2 in WT kidneys, but not in STC1 Tg kidneys (Fig. 8). These data are consistent with our hypothesis that STC1 suppresses the generation of free radicals, a mechanism that may underlie the resistance of STC1 Tg mice to I/R.

STC1 protects from I/R kidney injury through suppression of oxidant stress

STC1 decreases superoxide generation in many cells, including endothelial cells and macrophages [20;22], and our current data show that kidney I/R in STC1 Tg mice does not increase superoxide and H_2O_2. Therefore, we hypothesized that suppression of free radicals by STC1 may play a critical role in the protection from I/R kidney injury. Indeed, pre-treatment of STC1 Tg mice with paraquat (catalyzes the generation of superoxide) at a low dose which does not produce kidney injury by itself [see Fig. 9 and ref. [44]] before clamping, recapitulated the results observed in WT mice after I/R. As shown in Fig. 9, administration of paraquat to STC1 Tg mice before I/R is followed by: increased levels of superoxide (Fig. 9A) and H_2O_2 (Fig. 9B) in the kidneys at the 24h through the 72h time points post I/R; drop in CrCl at the 72h post I/R (Fig. 9C), and morphological changes in the kidneys similar to those observed in WT kidneys after I/R (Fig. 9D). On the other hand, pre-treatment of STC1 Tg mice with saline before I/R did not produce any of these changes. Consistent with previously published data [44], treatment of STC1 Tg mice with low dose paraquat alone did not produce kidney injury (Fig. 9C and Fig. 9D). Our data suggest that suppression of free radicals by STC1 is a primary mechanism for protection from I/R kidney injury.

Increased expression of UCP2 in tubular epithelium of STC1 Tg kidneys correlates with lower superoxide generation

STC1 Tg mice used for the current experiments display high circulating levels of STC1 protein and preferential expression of STC1 transgene in endothelial cells of the kidney [30;45]. STC1 is a secreted protein and functions in an autocrine/paracrine manner, and because of the juxtaposition of peritubular capillaries to epithelial cells, it is expected to act on neighboring epithelial cells, whether the protein originates from the circulation, or endothelial cells in the peritubular capillaries. In macrophages, STC1 suppresses superoxide generation through induction of UCP2 [22]. In the current experiment, we sought to determine UCP2 expression in the kidney using immunohistochemistry, and found higher level expression of the protein in tubular epithelial cells of STC1 Tg mice at baseline, compared with WT mice (Fig. 10), and incubation of kidney slices with MitoSOX reveals lower baseline levels of superoxide in tubule cells of STC1 Tg kidneys compared to WT kidneys (Fig. 10). The data are consistent with STC1-induced and UCP2-mediated tubular cell protection from oxidant stress in STC1 Tg kidneys.

Discussion

While a significant progress has been made in defining the pathophysiology of ischemic kidney injury, the therapeutic options for this disease remain limited. Our study demonstrates resistance of STC1 Tg mice to I/R, as we observe no significant change in:

CrCl; tubular morphology; infiltration with macrophages and T-cells; vascular permeability; production of superoxide and H_2O_2; and the activities of MAPKs. How might this resistance be conferred? A recent study showed dramatic increase in oxidative stress in critically ill humans with acute kidney failure, as evidenced by depletion of plasma thiols and increased formation of carbonyl [46]. Animal studies suggest that during ischemia, ATP is degraded to hypoxanthine; and after restoration of oxygen supply to the ischemic kidney, hypoxanthine is converted to xanthine by xanthine oxidase - generating superoxide and H_2O_2 in the process [47]. In the presence of iron, H_2O_2 forms hydroxyl radicals, which are highly reactive [48]. ROS cause cell injury by oxidation of proteins, peroxidation of lipids, and DNA damage, eventually causing cell death [49;50]. Indeed, administration of the superoxide scavenger, superoxide dismutase, before renal artery clamping and again prior to release of the clamp protects from I/R kidney injury [50]. These findings strongly suggest a primary role for free radicals in the pathogenesis of ischemic AKI. Similarly, our findings suggest that, inhibition of free radicals by STC1 is critical for the resistance displayed by STC1 Tg mice to I/R kidney injury, as administration of paraquat (a superoxide generator) to STC1 Tg mice before clamping of the renal pedicles, recapitulates the results observed in WT kidneys after renal pedicles clamping.

I/R kidney injury results from a dynamic and complex interaction between the vasculature and the tubules whereby vascular events alter oxygen and nutrient delivery to the epithelial cells, while the injured epithelium responds by producing autocrine/paracrine factors and cytokines which affect the survival of epithelial cells, and impact kidney function [51]. Recent observations by Brodsky et. al. [9] strongly suggest that endothelial cell dysfunction is the primary cause of cortical peritubular capillary noflow phenomenon which follows I/R, and prevention of endothelial insult protects from AKI. In cytokine-treated endothelial cells, we have previously shown STC1: blocks superoxide generation [20]; preserves endothelial barrier function [20]; and decreases transendothelial migration of leukocytes [21]. On the other hand, treatment of macrophages with STC1 diminishes the response to chemoattractants [23] and suppresses superoxide generation through induction of mitochondrial UCP2 [22]. It is worth noting again that kidneys of STC1 Tg mice used in our experiments display preferential expression of STC1 transgene in endothelial cells and macrophages [30], and our data reveal no change in vascular permeability in the kidneys of STC1 Tg mice after I/R injury, suggesting that STC1 protects endothelial cells *in vivo* as well. Is overexpression of STC1 in endothelial cells sufficient for renal protection from I/R? The answer to this question may not be easy to determine, because STC1 is a secreted protein and functions in an autocrine/paracrine manner; hence, limiting the effect of STC1 to a single cell type will be difficult. STC1 produced by endothelial cells is expected to act on neighboring cells; and because of the juxtaposition of epithelial cells to peritubular capillaries, it is highly likely that epithelial cells are exposed to STC1, whether the protein originates from endothelial cells in the peritubular capillaries, or the circulation, where high levels of STC1 exist in this Tg mouse line. Because STC1 induces uncoupling proteins [19;22], we examined the expression of UCP2, the prevailing uncoupling protein in the kidney, and found higher level expression of UCP2 in tubular epithelial cells of STC1 Tg kidneys, and as expected, incubation of kidney slices with MitoSOX reveals lower baseline levels of superoxide in tubule cells of STC1 Tg kidneys compared with WT kidneys,

consistent with a mechanism of action for STC1-induced and UCP2-mediated suppression of superoxide generation in epithelial cells.

It was traditionally thought that uncoupling of the mitochondria increases the generation of ROS. The evidence suggests otherwise. A group of UCP1 homologues has been discovered recently [UCP2 in the lymphoid system and kidney; UCP3 in the heart and skeletal muscle; UCP4 and UCP5 in the brain [52–54]], and like pharmacologic uncouplers [55], they diminish superoxide generation [52;53;56]. Consistent with these observations, increased expression of UCP2 in tubular epithelial cells suppresses the generation of ROS. Therefore, it is likely that the resistance to I/R kidney injury displayed by STC1 Tg mice is mediated through action of STC1 to protect the epithelium from oxidant injury, and preserve endothelial barrier function; but in addition, we can't dismiss possible contribution of STC1 action to inhibit macrophages. However; irrespective of how STC1 works, our data identify STC1 as an inducer of antioxidant pathway(s), relevant to the pathogenesis of I/R kidney injury, and suggest that STC1 may be an important therapeutic target for the management of ischemic injury in the kidney and other organs.

To illustrate the efficacy of a particular maneuver in the setting of I/R, studies usually focus on a single experimental variable under conditions where the severity of injury is optimal; this approach has demonstrated limited yield thus far. To complicate things further, protective actions attributed to parenchymal cells may be mediated through effects on the epithelium, the endothelium, or both, and demonstration of effects on proximal tubules doesn't necessarily mean they are limited to this site. For example; treatment of rats with Tin induces heme oxygenase and protects from I/R kidney injury; and while the expression of heme oxygenase is highest in cortical proximal tubules, global tubule cell protection in the outer medulla is observed [57], suggesting that endothelial expression of heme oxygenase or other factors may contribute to the protection in this setting [58]. Thus, successful treatment of ischemic AKI requires taking into account the complexity of this process, and requires the deployment of multi-pronged approaches - targeting key cells or processes that play important roles in the pathogenesis of I/R as is the case with STC1 protein.

Materials and methods

Materials

All materials were purchased from Sigma (St Louis, MO) unless stated otherwise. MitoSOX was purchased from Invitrogen (Carlsbad, CA). Creatinine measurement kit was purchased from Abcam (Cambridge, MA). Goat anti-UCP2 was purchased from Lifespan Biosciences (Seattle, WA). Goat anti-hSTC1 antibodies were purchased from Santa-Cruz (Santa Cruz, CA); rabbit anti-STC1 antibodies were a gift from Dr Gert Flik [59]. Rabbit anti-ERK, rabbit anti-p-ERK, rabbit anti-JNK, rabbit anti-p-JNK, rabbit anti-p38 kinase, and rabbit anti-p-p38 kinase were purchased from Cell Signaling (Danvers, MA). Rabbit anti-actin was purchased from Sigma; rat anti-F4/80, rat anti-mouse CD3 and rat anti-CD68 were purchased from AbD Serotec (Raleigh, NC). Fluorescein isothiocyanate (FITC)-labeled anti-goat antibody was purchased from Invitrogen (Carlsbad, CA).

Mice

STC1 Tg mice were generated by Varghese et al. [45], and made available for our studies. STC1 transgene is driven by the metallothionein I minimal promoter over C57B/6 genetic background [45]. Transgenic mice are 30–40% smaller in size-relative to WT litter-mates [45] and display: elevated serum STC1 and normal serum calcium [45]. Blood pressure is normal [30], as well as hematocrit (50% WT, 52% STC1 Tg; P=NS) and baseline serum creatinine (0.10 ± 0.004 mg/dL WT, 0.11 ± 0.016 mg/dL STC1 Tg; P=NS). Of note, STC1 expression in the kidneys of STC1 Tg mice is similar to that of WT mice, except for higher expression in endothelial cells and macrophages [30]. All studies were carried out using mice homozygous for the transgene [derived from line 2; [45]] and WT mice generated from crosses between mice heterozygous for the transgene. Mice were maintained in air conditioned rooms under pathogen-free conditions with 12h/12h light/dark cycles, and were given free access to food and water during the experiments. The investigation conforms to the Guide for the Care and Use of Laboratory Animals published by the US National Institutes of Health (NIH Publication No. 85–23, revised 1996), and animal experiments were approved by university ethics review board.

AKI model

We used an established mouse model of kidney I/R injury induced by clamping of bilateral renal pedicles [60]. Briefly, male and female mice (12–20 wks, 22–25g) were anesthetized with an i.p. injection of 2 mL/kg of combination anesthetic (contains/1 mL: ketamine 37.5 mg, Xylazine 1.9 mg and acepromazine 0.37 mg). Following abdominal incision, left and right renal pedicles were bluntly dissected and a non-traumatic vascular clamp (Roboz Surgical Instruments) was placed on each renal pedicle for 30 min. During the procedure, animals were kept under heating lamp and hydrated with warm saline. After 30 min of ischemia, the clamps were removed, the wounds sutured, and the animals were allowed to recover. Sham-treated animals underwent similar surgical procedures without clamping of the renal pedicles. For some experiments, a portion of STC1 Tg mice were given a single i.p. injection of saline or paraquat at 12.5 mg/kg, 2h before clamping/sham surgery. Mice were sacrificed at 24h, 48h, 72h or 8d after surgical procedure, blood samples were obtained via cardiac puncture (for creatinine measurement) and kidneys were harvested for analysis of: histology; immunohistochemistry; Western blotting to assess the activities of MAPKs and STC1 protein expression; superoxide and H_2O_2. Before sacrifice, a timed urine collection was obtained for calculation of CrCl. Because of the sexual dimorphism in the susceptibility to I/R kidney injury [61–63], we included both genders in our studies – to determine the impact of STC1 on the post-I/R phenotype in male and female mice.

Assessment of renal function

For timed urine collection, mice were placed in metabolic cages for 20h before sacrifice. Serum creatinine was measured using capillary electrophoresis method (courtesy of the Physiology Core lab, O'Brien Kidney Center, University of Texas Southwestern Medical Center, Dallas, TX). Urine creatinine was measured using Abcam Inc. creatinine assay kit, as per manufacturer's instructions, and the results were verified by parallel measurements of

random samples using the hospital clinical lab. CrCl was calculated and normalized to weight.

Vascular permeability

Five hours after I/R (optimal, based on time course), mice were given 2% Evans blue dye (0.5 mg/25 μL/g weight) in phosphate buffered saline [(PBS); composition: 3.2 mM Na_2HPO_4; 0.5 mM KH_2PO_4; 1.3 mM KCl; 135 mM NaCl; pH 7.4], delivered through the tail vein. Five min after dye injection, mice were anesthetized and perfused with PBS continuously for 20 min through cardiac puncture. Kidneys were removed, weighed, and suspended in cold PBS (1g tissue/3 mL buffer), homogenized using MAX Digital High Viscosity Mixer (Henry Troemner LLC.; Thorofare, NJ) and Kontes Glass Duall® tissue grinder (size 21; Fisher Scientific, Pittsburgh, PA), and centrifuged for 20 min at 4 C, 10,000 rpm, on bench top centrifuge. The supernatant was recovered and the pellet was washed in PBS and centrifuged again as above, followed by recovery of the second supernatant. Pooled supernatants were treated with deoxycholic acid (1% final) to decrease turbidity secondary to lipids (opaque supernatant), and absorbance was measured at 540 nm (represents retention of Evans blue in the kidney, and corresponds to vascular permeability).

Immunohistochemistry

Frozen or Methanol-Carnoy (Methacarn)-fixed kidney sections (4-μm) were subjected to: Periodic Acid Schiff (PAS) staining (for morphology); anti-F4/80; anti-CD68 (pan-macrophage marker); anti-CD3 (lymphocytes); anti-p-p38 (active kinase); anti-p-ERK (active kinase); anti-p-JNK (active kinase); anti-STC1; or anti-UCP2. Detection was carried out using peroxidase enzyme-based detection system (Vector Laboratories) or FITC-labeled secondary antibody for UCP2. Photomicrographs were taken using Nikon Eclipse 80i microscope system. Total macrophages ($CD68^+$), resident macrophages/dendritic cells ($F4/80^+$), and T cells ($CD3^+$) infiltrating the interstitium in an area spanning the inner cortex and cortico-medullary junction were counted, and the results were expressed as the means and standard error of means (± SEM) of positively stained cells in 10 grids (1-cm^2 graded ocular grids viewed at × 20 magnification).

In situ activity of MAPKs

Tubular or interstitial cells positively stained for active kinases p-ERK, p-JNK or p-p38 kinase were counted as above.

Sodium dodecyl sulfate-polyacrylamide gel electrophoresis (SDS-PAGE)

lysates representing whole kidney from WT or STC1 Tg mice [45], were suspended in modified radioimmunoprecipitation assay (RIPA) buffer [composition: 150 mM NaCl; 50 mM Tris-HCl (pH 7.4); 1% NP-40; 0.25% sodium deoxycholate; 1 mM ethylenediaminetetraacetic acid (EDTA); 1x cocktail proteinase inhibitors], and centrifuged at 8000 g for 10 min, 4°C, to remove cell debris. Fifty μg representing whole kidney protein were resolved on 12% SDS-PAGE, transferred to nitrocellulose membrane and incubated with primary antibodies for: STC1, ERK; p-ERK; JNK; p-JNK; p38 kinase or p-p38 kinase. After washing with PBS containing 0.1% Tween-20, the membrane was incubated with

horse radish peroxidase-conjugated secondary antibody. The bound antibodies were visualized using chemiluminescence.

Superoxide measurements

Twenty four hours after I/R, kidneys were harvested and homogenized (as above) in 500 μL sucrose buffer (composition: 0.31 M sucrose; 10 mM Tris-HCl; pH 7.4) on ice, followed by protein quantitation (Bradford's method). Kidney lysates (100 μg protein/100 μL) were placed in clear flat-bottom wells (96-well plate), containing excess dihydroethidium (DHE; 100 μM), in a final volume of 100 μL. The absorbance (excitation at 530 nm, and emission at 620 nm) was immediately measured. Absorbance values were normalized to the absorbance of wells containing equimolar concentrations of DHE alone, and expressed as OD/μg protein.

H_2O_2 measurements

Twenty four hours after I/R, kidneys were harvested and homogenized (as above) in 500 μL sucrose buffer on ice, followed by protein quantitation (Bradford's method). H_2O_2 was measured as described by Jiang et al. [64]. The method takes advantage of the conversion of Fe^{2+} to Fe^{3+} in the presence of H_2O_2; followed by detection of Fe^{3+}-xylenol orange complex. Briefly, kidney lysate (100 μg/20 μL), was added to 180 μL assay buffer (composition: 100 μM xylenol orange; 250 μM ammonium ferrous sulfate; 4 mM butylated hydroxytoluene; 25 mM H_2SO_4; in methanol), incubated at RT for 30 min, followed by measurement of absorbance at 560 nm. Absorbance values were normalized to the absorbance of wells containing assay buffer alone, and expressed as OD/mg protein.

MitoSOX fluorescence

Freshly isolated kidneys were sectioned coronally to obtain one mm thick slices that were incubated in PBS containing 5 μM MitoSOX™ Red reagent for 10 min. MitoSOX permeates live cells and selectively targets the mitochondria. It is rapidly oxidized by superoxide and emits red fluorescence. Following incubation with MitoSOX, kidney slices were rinsed in PBS, fixed in 4% paraformaldehyde, imbedded in paraffin and 5 μM sections were viewed under fluorescence microscope.

MAPKs activities in whole kidney

Whole kidney lysates were resolved on 12% SDS-PAGE and Western blots were reacted with MAPKs Abs followed by stripping and reaction with phospho-MAPKs Abs. Bands representing phospho-MAPKs were normalized to the corresponding bands representing total MAPKs (p-ERK/ERK; p-JNK/JNK; p-p38/p38), and expressed as means ± SEM of 3–5 independent determinations.

Statistics

Data are expressed as means ± SEM and are compared by one way ANalysis Of VAriance (ANOVA) for three or more groups, or unpaired t-test. Statistical significance of difference was defined by a *p*-value of less than 0.05.

Acknowledgments

Funding: This work was supported by grants from the National Institute of Diabetes and Digestive and Kidney Diseases at the National Institutes of Health [R01 DK080306; T32 DK062706].

Abbreviations

I/R	ischemia/reperfusion
STC1	stanniocalcin-1
WT	wild type
CrCl	creatinine clearance
Tg	transgenic
UCP	uncoupling protein
AKI	acute kidney injury
MCP-1	macrophage chemotactic protein-1
TNF-1α	tumor necrosis factor-1α
MAPK	mitogen activated protein kinase
ERK	extracellular regulated kinase
JNK	June N-terminal kinase
p38	p38 kinase
NF-κB	Nuclear Factor-κB
ROS	reactive oxygen species
CD3	a marker of T-cells
F4/80	a marker of macrophage and dendritic cells
CD68	pan-macrophage marker
FITC	Fluorescein isothiocyanate
PBS	phosphate buffered saline
Methacarn	Methanol-Carnoy
PAS	periodic acid Schiff
SDS	sodium dodecyl sulfate
PAGE	polyacrylamide gel electrophoresis
EDTA	ethylenediaminetetraacetic acid
DHE	dihydroethidium

References

1. Gueler F, Gwinner W, Schwarz A, Haller H. Long-term effects of acute ischemia and reperfusion injury. Kidney Int. 2004; 66:523–527. [PubMed: 15253702]

2. Halloran PF, Homik J, Goes N, et al. The "injury response": a concept linking nonspecific injury, acute rejection, and long-term transplant outcomes. Transplant Proc. 1997; 29:79–81. [PubMed: 9123164]

3. Lassnigg A, Schmidlin D, Mouhieddine M, et al. Minimal changes of serum creatinine predict prognosis in patients after cardiothoracic surgery: a prospective cohort study. J Am Soc Nephrol. 2004; 15:1597–1605. [PubMed: 15153571]

4. Loef BG, Epema AH, Smilde TD, et al. Immediate postoperative renal function deterioration in cardiac surgical patients predicts in-hospital mortality and long-term survival. J Am Soc Nephrol. 2005; 16:195–200. [PubMed: 15563558]

5. Chertow GM, Burdick E, Honour M, et al. Acute kidney injury, mortality, length of stay, and costs in hospitalized patients. J Am Soc Nephrol. 2005; 16:3365–3370. [PubMed: 16177006]

6. Devarajan P. Cellular and molecular derangements in acute tubular necrosis. Curr Opin Pediatr. 2005; 17:193–199. [PubMed: 15800411]

7. Molitoris BA, Sandoval R, Sutton TA. Endothelial injury and dysfunction in ischemic acute renal failure. Crit Care Med. 2002; 30:S235–S240. [PubMed: 12004242]

8. Sutton TA, Mang HE, Campos SB, et al. Injury of the renal microvascular endothelium alters barrier function after ischemia. Am J Physiol Renal Physiol. 2003; 285:F191–F198. [PubMed: 12684225]

9. Brodsky SV, Yamamoto T, Tada T, et al. Endothelial dysfunction in ischemic acute renal failure: rescue by transplanted endothelial cells. Am J Physiol Renal Physiol. 2002; 282:F1140–F1149. [PubMed: 11997331]

10. Jang HR, Ko GJ, Wasowska BA, Rabb H. The interaction between ischemia-reperfusion and immune responses in the kidney. J Mol Med. 2009; 87:859–864. [PubMed: 19562316]

11. Day YJ, Huang L, Ye H, et al. Renal ischemia-reperfusion injury and adenosine 2A receptor-mediated tissue protection: role of macrophages. Am J Physiol Renal Physiol. 2005; 288:F722–F731. [PubMed: 15561971]

12. Vinuesa E, Hotter G, Jung M, et al. Macrophage involvement in the kidney repair phase after ischaemia/reperfusion injury. J Pathol. 2008; 214:104–113. [PubMed: 17973244]

13. Jo SK, Sung SA, Cho WY, et al. Macrophages contribute to the initiation of ischaemic acute renal failure in rats. Nephrol Dial Transplant. 2006; 21:1231–1239. [PubMed: 16410269]

14. Lee S, Huen S, Nishio H, et al. Distinct macrophage phenotypes contribute to kidney injury and repair. J Am Soc Nephrol. 2011; 22:317–326. [PubMed: 21289217]

15. Beck-Schimmer B, Oertli B, Pasch T, Wuthrich RP. Hyaluronan induces monocyte chemoattractant protein-1 expression in renal tubular epithelial cells. J Am Soc Nephrol. 1998; 9:2283–2290. [PubMed: 9848782]

16. Dong X, Swaminathan S, Bachman LA, et al. Resident dendritic cells are the predominant TNF-secreting cell in early renal ischemia-reperfusion injury. Kidney Int. 2007; 71:619–628. [PubMed: 17311071]

17. Mehta A, Sekhon CP, Giri S, et al. Attenuation of ischemia/reperfusion induced MAP kinases by N-acetyl cysteine, sodium nitroprusside and phosphoramidon. Mol Cell Biochem. 2002; 240:19–29. [PubMed: 12487368]

18. Park KM, Chen A, Bonventre JV. Prevention of kidney ischemia/reperfusion-induced functional injury and JNK, p38, and MAPK kinase activation by remote ischemic pretreatment. J Biol Chem. 2001; 276:11870–11876. [PubMed: 11150293]

19. Sheikh-Hamad D. Mammalian stanniocalcin-1 activates mitochondrial antioxidant pathways: new paradigms for regulation of macrophages and endothelium. Am J Physiol Renal Physiol. 2010; 298:F248–F254. [PubMed: 19656913]

20. Chen C, Jamaluddin MS, Yan S, et al. Human stanniocalcin-1 blocks TNF-alpha-induced monolayer permeability in human coronary artery endothelial cells. Arterioscler Thromb Vasc Biol. 2008; 28:906–912. [PubMed: 18309109]

21. Chakraborty A, Brooks H, Zhang P, et al. Stanniocalcin-1 regulates endothelial gene expression and modulates transendothelial migration of leukocytes. Am J Physiol Renal Physiol. 2007; 292:F895–F904. [PubMed: 17032941]

22. Wang Y, Huang L, Abdelrahim M, et al. Stanniocalcin-1 suppresses superoxide generation in macrophages through induction of mitochondrial UCP2. J Leukoc Biol. 2009; 86:981–988. [PubMed: 19602668]
23. Kanellis J, Bick R, Garcia G, et al. Stanniocalcin-1, an inhibitor of macrophage chemotaxis and chemokinesis. Am J Physiol Renal Physiol. 2004; 286:F356–F362. [PubMed: 14570698]
24. De Niu P, Radman DP, Jaworski EM, et al. Development of a human stanniocalcin radioimmunoassay: serum and tissue hormone levels and pharmacokinetics in the rat. Mol Cell Endocrinol. 2000; 162:131–144. [PubMed: 10854706]
25. Jellinek DA, Chang AC, Larsen MR, et al. Stanniocalcin 1 and 2 are secreted as phosphoproteins from human fibrosarcoma cells. Biochem J. 2000; 350(Pt 2):453–461. [PubMed: 10947959]
26. Zhang J, Alfonso P, Thotakura NR, et al. Expression, purification, and bioassay of human stanniocalcin from baculovirus-infected insect cells and recombinant CHO cells. Protein Expr Purif. 1998; 12:390–398. [PubMed: 9535707]
27. Luo CW, Kawamura K, Klein C, Hsueh AJ. Paracrine regulation of ovarian granulosa cell differentiation by stanniocalcin (STC) 1: mediation through specific STC1 receptors. Mol Endocrinol. 2004; 18:2085–2096. [PubMed: 15131261]
28. Block GJ, Ohkouchi S, Fung F, et al. Multipotent stromal cells are activated to reduce apoptosis in part by upregulation and secretion of stanniocalcin-1. Stem Cells. 2009; 27:670–681. [PubMed: 19267325]
29. James K, Seitelbach M, McCudden CR, Wagner GF. Evidence for stanniocalcin binding activity in mammalian blood and glomerular filtrate. Kidney Int. 2005; 67:477–482. [PubMed: 15673295]
30. Huang L, Garcia G, Lou Y, et al. Anti-inflammatory and renal protective actions of stanniocalcin-1 in a model of anti-glomerular basement membrane glomerulonephritis. Am J Pathol. 2009; 174:1368–1378. [PubMed: 19246645]
31. McCudden CR, James KA, Hasilo C, Wagner GF. Characterization of mammalian stanniocalcin receptors. Mitochondrial targeting of ligand and receptor for regulation of cellular metabolism. J Biol Chem. 2002; 277:45249–45258. [PubMed: 12223480]
32. Re RN, Cook JL. The mitochondrial component of intracrine action. Am J Physiol Heart Circ Physiol. 2010; 299:H577–H583. [PubMed: 20622110]
33. Molitoris BA, Hoilien CA, Dahl R, et al. Characterization of ischemia-induced loss of epithelial polarity. J Membr Biol. 1988; 106:233–242. [PubMed: 2468776]
34. Khundmiri SJ, Asghar M, Khan F, et al. Effect of reversible and irreversible ischemia on marker enzymes of BBM from renal cortical PT subpopulations. Am J Physiol. 1997; 273:F849–F856. [PubMed: 9435672]
35. Thornton MA, Winn R, Alpers CE, Zager RA. An evaluation of the neutrophil as a mediator of in vivo renal ischemic-reperfusion injury. Am J Pathol. 1989; 135:509–515. [PubMed: 2782382]
36. Linas SL, Shanley PF, Whittenburg D, et al. Neutrophils accentuate ischemia-reperfusion injury in isolated perfused rat kidneys. Am J Physiol. 1988; 255:F728–F735. [PubMed: 2845813]
37. Linfert D, Chowdhry T, Rabb H. Lymphocytes and ischemia-reperfusion injury. Transplant Rev (Orlando). 2009; 23:1–10. [PubMed: 19027612]
38. Pombo CM, Bonventre JV, Avruch J, et al. The stress-activated protein kinases are major c-Jun amino-terminal kinases activated by ischemia and reperfusion. J Biol Chem. 1994; 269:26546–26551. [PubMed: 7929379]
39. di Mari JF, Davis R, Safirstein RL. MAPK activation determines renal epithelial cell survival during oxidative injury. Am J Physiol. 1999; 277:F195–F203. [PubMed: 10444573]
40. Meldrum KK, Meldrum DR, Hile KL, et al. p38 MAPK mediates renal tubular cell TNF-alpha production and TNF-alpha-dependent apoptosis during simulated ischemia. Am J Physiol Cell Physiol. 2001; 281:C563–C570. [PubMed: 11443055]
41. Nguyen A, Chang AC, Reddel RR. Stanniocalcin-1 acts in a negative feedback loop in the prosurvival ERK1/2 signaling pathway during oxidative stress. Oncogene. 2009; 7(28(18)):1982–1992. [PubMed: 19347030]
42. Boueiz A, Hassoun PM. Regulation of endothelial barrier function by reactive oxygen and nitrogen species. Microvasc Res. 2009; 77:26–34. [PubMed: 19041330]

43. Devarajan P. Update on mechanisms of ischemic acute kidney injury. J Am Soc Nephrol. 2006; 17:1503–1520. [PubMed: 16707563]
44. Cheng WH, Ho YS, Valentine BA, et al. Cellular glutathione peroxidase is the mediator of body selenium to protect against paraquat lethality in transgenic mice. J Nutr. 1998; 128:1070–1076. [PubMed: 9649587]
45. Varghese R, Gagliardi AD, Bialek PE, et al. Overexpression of human stanniocalcin affects growth and reproduction in transgenic mice. Endocrinology. 2002; 143:868–876. [PubMed: 11861508]
46. Himmelfarb J, McMonagle E, Freedman S, et al. Oxidative stress is increased in critically ill patients with acute renal failure. J Am Soc Nephrol. 2004; 15:2449–2456. [PubMed: 15339994]
47. Linas SL, Whittenburg D, Repine JE. Role of xanthine oxidase in ischemia/reperfusion injury. Am J Physiol. 1990; 258:F711–F716. [PubMed: 2316673]
48. Granger DN. Role of xanthine oxidase and granulocytes in ischemia-reperfusion injury. Am J Physiol. 1988; 255:H1269–H1275. [PubMed: 3059826]
49. Erdogan H, Fadillioglu E, Yagmurca M, et al. Protein oxidation and lipid peroxidation after renal ischemia-reperfusion injury: protective effects of erdosteine and N-acetylcysteine. Urol Res. 2006; 34:41–46. [PubMed: 16429300]
50. Paller MS, Hoidal JR, Ferris TF. Oxygen free radicals in ischemic acute renal failure in the rat. J Clin Invest. 1984; 74:1156–1164. [PubMed: 6434591]
51. Bonventre JV, Weinberg JM. Recent advances in the pathophysiology of ischemic acute renal failure. J Am Soc Nephrol. 2003; 14:2199–2210. [PubMed: 12874476]
52. Brand MD, Esteves TC. Physiological functions of the mitochondrial uncoupling proteins UCP2 and UCP3. Cell Metab. 2005; 2:85–93. [PubMed: 16098826]
53. Kim-Han JS, Dugan LL. Mitochondrial uncoupling proteins in the central nervous system. Antioxid Redox Signal. 2005; 7:1173–1181. [PubMed: 16115020]
54. Echtay KS, Murphy MP, Smith RA, et al. Superoxide activates mitochondrial uncoupling protein 2 from the matrix side. Studies using targeted antioxidants. J Biol Chem. 2002; 277:47129–47135. [PubMed: 12372827]
55. Korshunov SS, Skulachev VP, Starkov AA. High protonic potential actuates a mechanism of production of reactive oxygen species in mitochondria. FEBS Lett. 1997; 416:15–18. [PubMed: 9369223]
56. Rousset S, Alves-Guerra MC, Mozo J, et al. The Biology of Mitochondrial Uncoupling Proteins. Diabetes. 2004; 53:S130–S135. [PubMed: 14749278]
57. Toda N, Takahashi T, Mizobuchi S, et al. Tin chloride pretreatment prevents renal injury in rats with ischemic acute renal failure. Crit Care Med. 2002; 30:1512–1522. [PubMed: 12130972]
58. Katori M, Busuttil RW, Kupiec-Weglinski JW. Heme oxygenase-1 system in organ transplantation. Transplantation. 2002; 74:905–912. [PubMed: 12394829]
59. Wendelaar Bonga SE, Smits PW, Flik G, et al. Immunocytochemical localization of hypocalcin in the endocrine cells of the corpuscles of Stannius in three teleost species (trout, flounder and goldfish). Cell Tissue Res. 1989; 255:651–656. [PubMed: 2706667]
60. Liu M, Chien CC, Grigoryev DN, et al. Effect of T cells on vascular permeability in early ischemic acute kidney injury in mice. Microvasc Res. 2009; 77:340–347. [PubMed: 19323971]
61. Kim J, Kil IS, Seok YM, et al. Orchiectomy attenuates post-ischemic oxidative stress and ischemia/reperfusion injury in mice. A role for manganese superoxide dismutase. J Biol Chem. 2006; 281:20349–20356. [PubMed: 16682413]
62. Muller V, Losonczy G, Heemann U, et al. Sexual dimorphism in renal ischemiareperfusion injury in rats: possible role of endothelin. Kidney Int. 2002; 62:1364–1371. [PubMed: 12234307]
63. Park KM, Cho HJ, Bonventre JV. Orchiectomy reduces susceptibility to renal ischemic injury: a role for heat shock proteins. Biochem Biophys Res Commun. 2005; 328:312–317. [PubMed: 15670785]
64. Jiang ZY, Woollard AC, Wolff SP. Hydrogen peroxide production during experimental protein glycation. FEBS Lett. 1990; 268:69–71. [PubMed: 2384174]

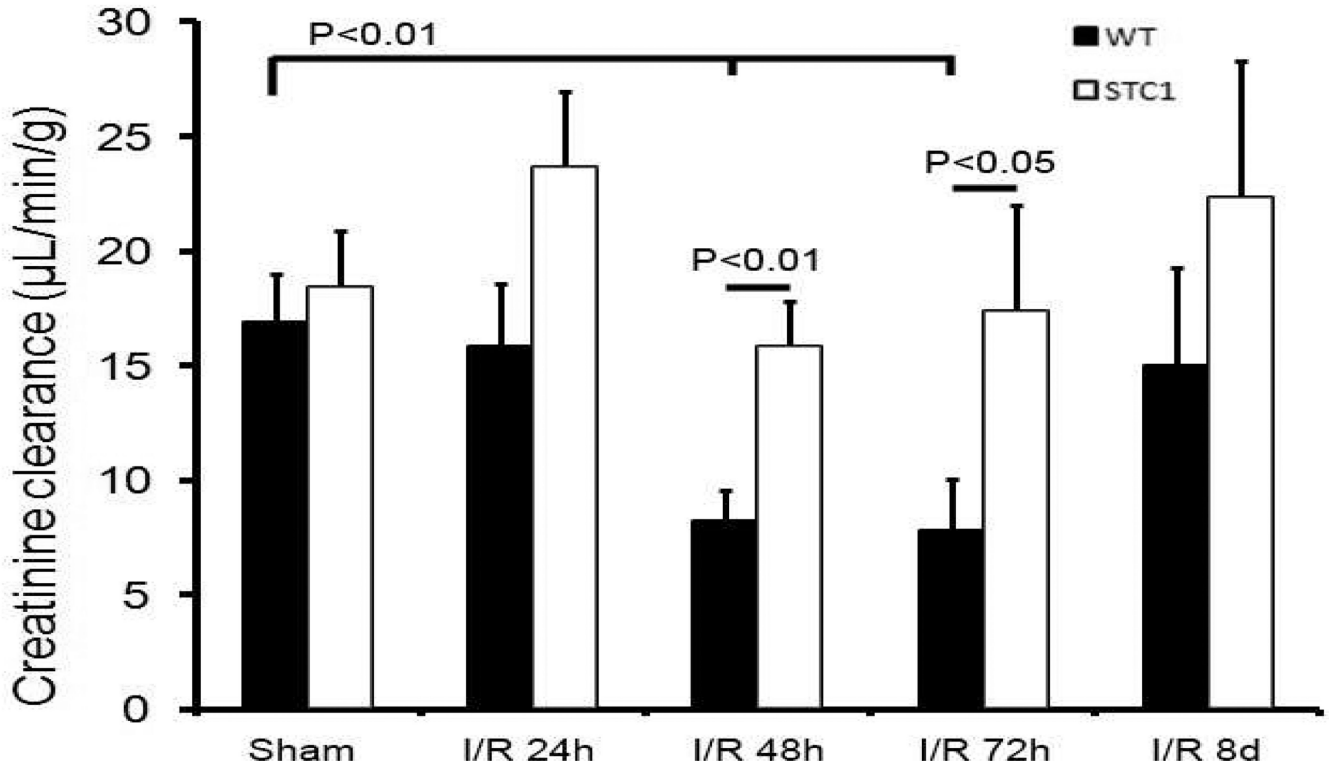

Figure 1. Transgenic overexpression of STC1 confers resistance to I/R kidney injury: STC1 Tg mice display no change in CrCl after I/R

Mice were killed 24h, 48h, 72h or 8d following I/R and blood samples were obtained for creatinine measurements. Timed urine collections, corresponding to the last 20h preceding the above time points were used for creatinine measurements and CrCl calculations normalized to weight. Bar graph represents values obtained from at least 6 mice for each group at every time point, except for sham bars which represent cumulative values from all sham treated mice at all time points (n≥24).

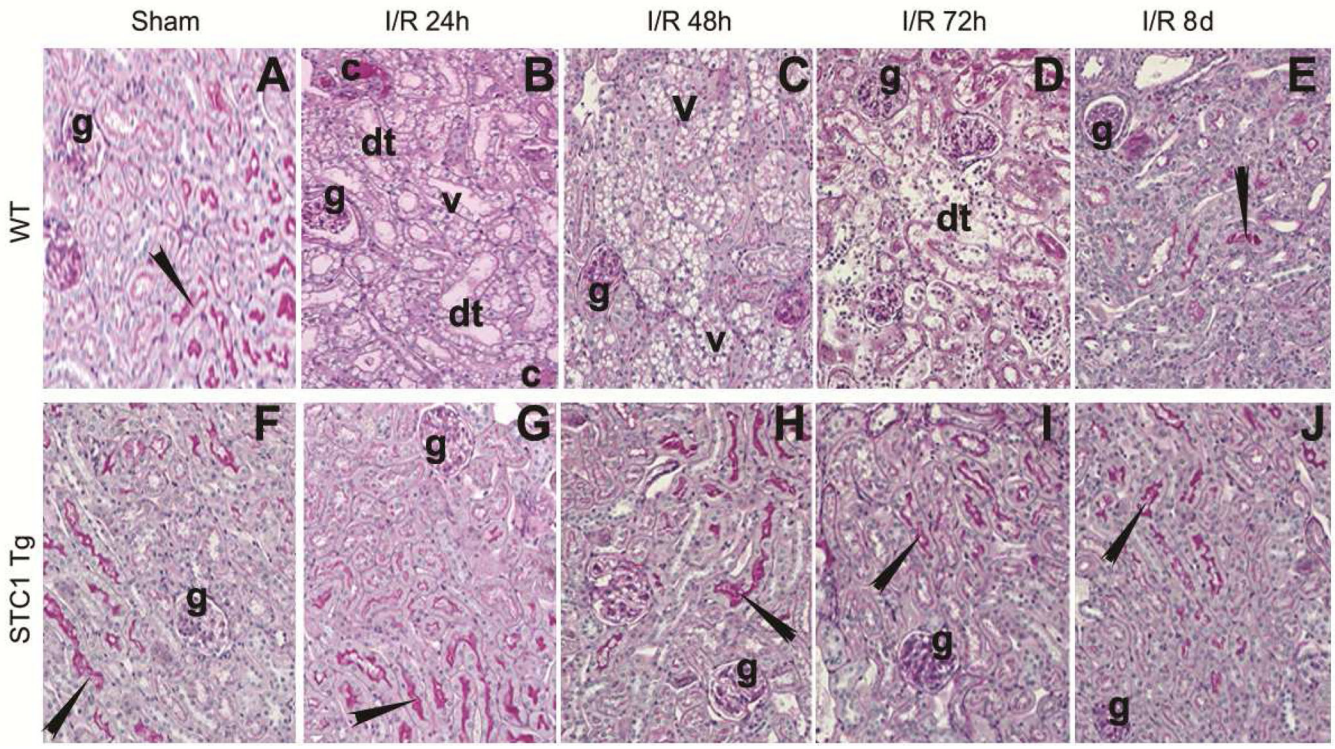

Figure 2. Transgenic overexpression of STC1 confers resistance to I/R kidney injury: STC1 Tg mice display no change in kidney morphology after I/R

Mice were killed 24h, 48h, 72h or 8d following I/R and kidneys were subjected to PAS staining. Following I/R and compared to sham-treated controls (**Fig. 2A**), WT mice displayed loss of brush border membrane (arrowheads), severe cellular vacuolization (v) and tubular dilatation (dt) with cast formation (c), starting 24h after I/R, persisting through the 72h time point (**Fig. 2B, 2C and 2D**). Glomeruli are marked by the letter "g". Recovery of morphology in WT kidneys is observed by day 8 (**Fig. 2E**). In contrast, following I/R and similar to sham treated controls (**Fig. 2F**), kidneys of STC1 Tg mice demonstrated morphological preservation of brush border membrane (arrowheads) throughout the time course, and showed no evidence of cellular vacuolization, tubular dilatation or cast formation (**Fig. G–J**). Representative images are shown (magnification 200X).

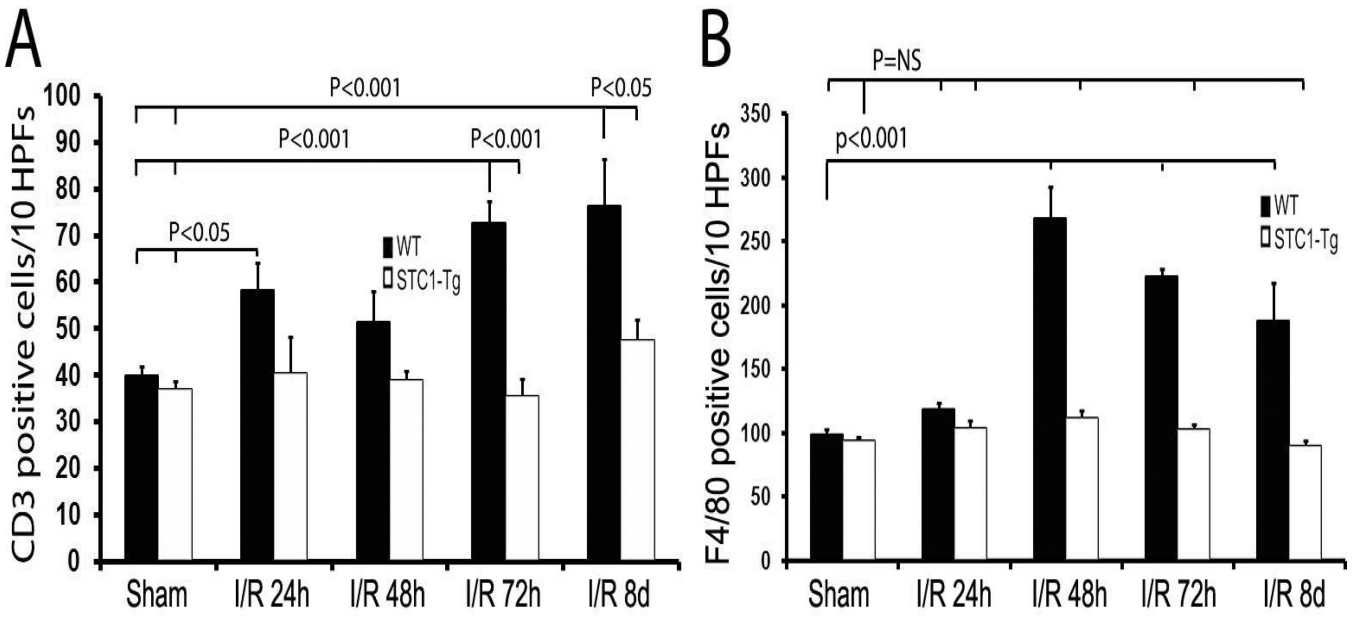

Figure 3. Increased expression of STC1 protein after I/R in injured tubules of WT kidneys

A. Mice were killed 24h following I/R and proteins representing whole kidney were resolved on SDS-PAGE; Western blots were reacted consecutively with anti-STC1 followed by β-actin, and the ratio of STC1/β-actin was calculated. Bar graph represents data from 6 mice for each group and depicts the mean (± SEM). **B.** Mice were killed 24h following I/R and Methacarn-fixed kidneys were subjected to staining with anti-STC1. WT kidneys displayed increased expression of STC1 in injured tubules (vacuolated cells) following I/R; whereas, staining for STC1 in Tg kidneys remained unchanged, and was prominent on the endothelial surface of arteries (a), interstitial venules (arrowheads), and capillaries in the glomeruli (g). Representative images are shown (magnification 200X).

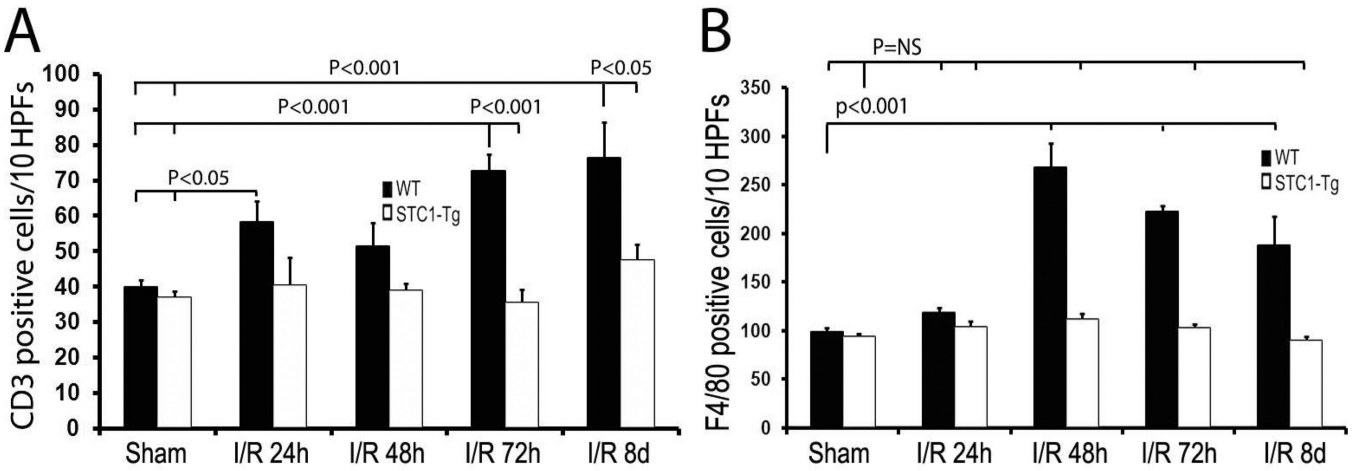

Figure 4. WT kidneys, but not STC1 Tg kidneys, demonstrate increased infiltration with macrophages and T-cells following I/R

Mice were killed 24h, 48h, 72h or 8d following I/R and kidney sections were stained with anti-CD3 or anti-F4/80. Bar graphs represent cumulative data obtained from at least 6 mice for each group/time point – where the mean (±SEM) of CD3 or F4/80 positively-stained cells infiltrating 10 grids spanning the inner cortex and cortico-medullary junction (1-cm^2 graded ocular grids viewed at magnification 200X) were counted. Following I/R and compared to sham-treated controls, WT kidneys displayed increased infiltration with T-cells (CD3+; Fig 4A) and macrophages (F4/80+; Fig 4B). In contrast, kidneys of STC1 Tg mice displayed no change in the number of T-cells or macrophages after I/R.

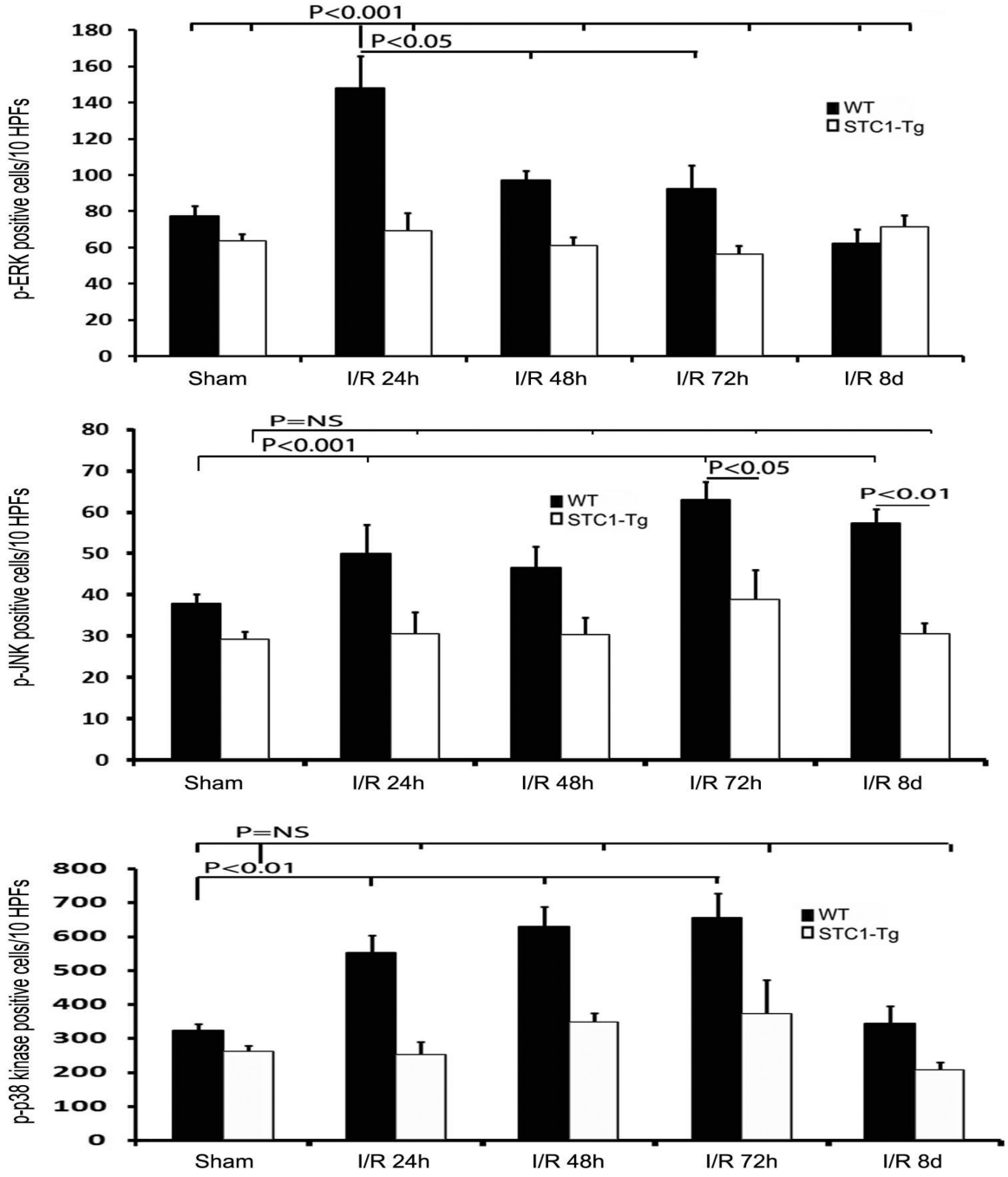

Figure 5. Increased number of cells with active MAPKs in the kidneys of WT mice after I/R, but not in the kidneys of STC1 Tg mice

Mice were killed 24h, 48h, 72h or 8d following I/R and kidney sections were stained with anti-p-ERK, anti-p-JNK or anti-p-p38 kinase. Bar graphs represent cumulative data obtained from at least 6 mice for each group/time point – where the mean (± SEM) of p-ERK, p-JNK or p-p38 kinase positively-stained cells in 10 grids (1-cm^2 graded ocular grids viewed at magnification 200X) spanning the inner cortex and cortico-medullary junction were counted. Following I/R and compared to sham-treated controls, WT kidneys displayed

increased number of cells positively stained for active MAPKs. In contrast, kidneys of STC1 Tg mice displayed no change in the number of cells positively stained for active MAPKs.

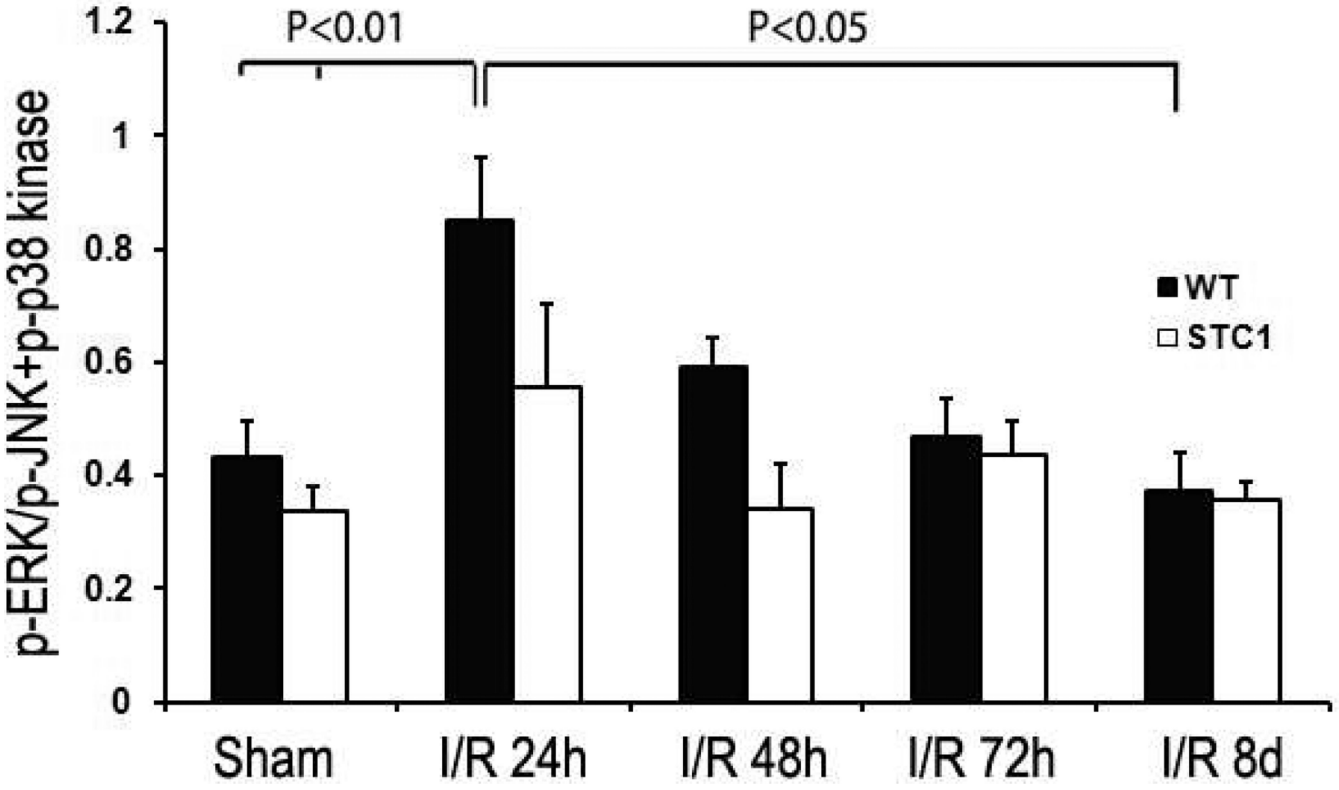

Figure 6. Higher p-ERK/p-p38+p-JNK in WT kidneys after I/R, compared with STC1 Tg kidneys

Mice were killed 24h, 48h, 72h or 8d following I/R and proteins representing whole kidney lysates were resolved on SDS-PAGE; Western blots were reacted consecutively with anti-MAPK followed by the respective anti-p-MAPK, and the ratio of p-MAPK/total MAPK was calculated. Bar graph represents data from 5–7 mice for each group/time point and depicts the mean (± SEM) of p-ERK/total ERK divided by the sum of p-JNK/total JNK plus p-p38/total p38. Data show higher p-ERK/p-JNK+p-p38 in WT kidney lysates at the 24h time point compared to STC1 Tg kidney lysates.

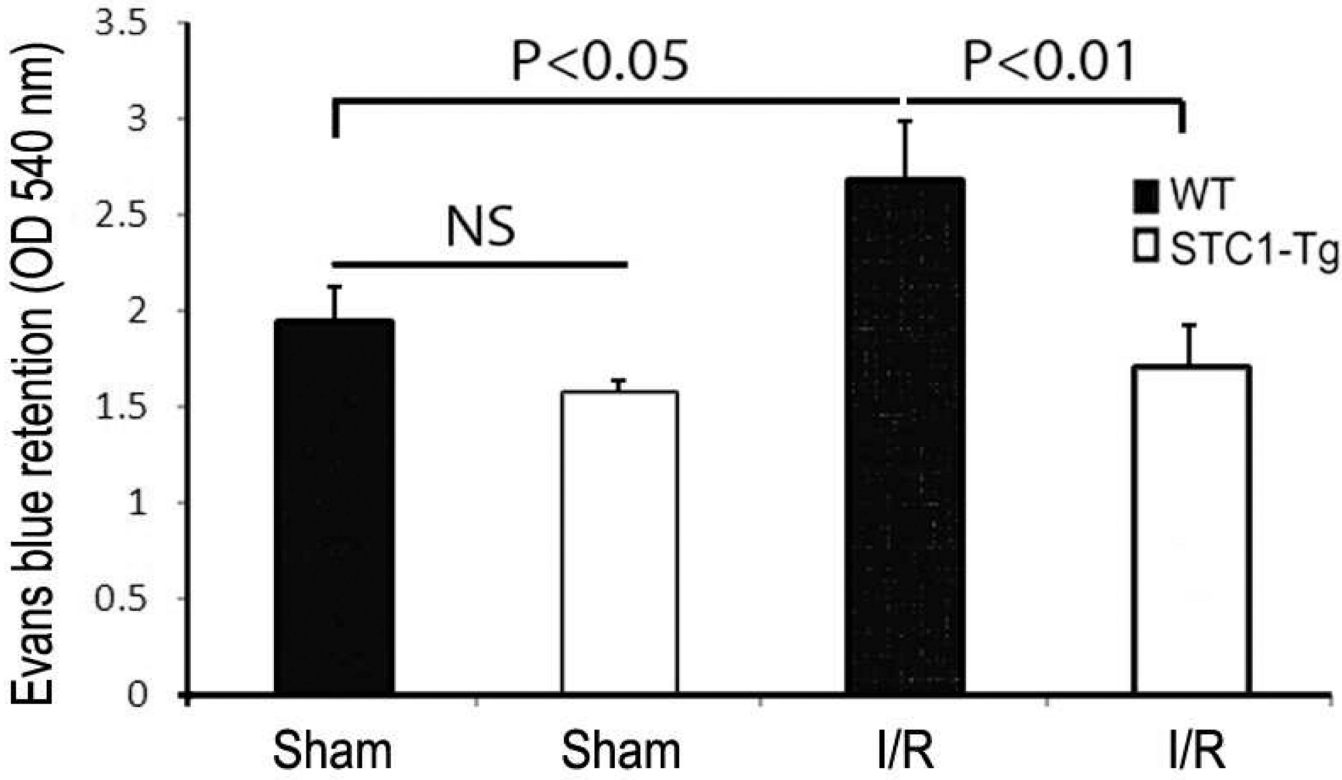

Figure 7. Increased vascular permeability after I/R injury in WT kidneys, but not in STC1 Tg kidneys

Five hours after I/R, mice were given an injection of 2% Evans blue dye through the tail vein. Mice were anesthetized five min after dye injection, and kidneys were perfused continuously with PBS for 20 minutes. Kidneys were then homogenized and dye retention was measured fluorometrically. Bar graphs represent the mean (± SEM) of data obtained from 9 mice for each group and show higher Evans blue retention in WT kidneys after I/R, but not in STC1 Tg kidneys.

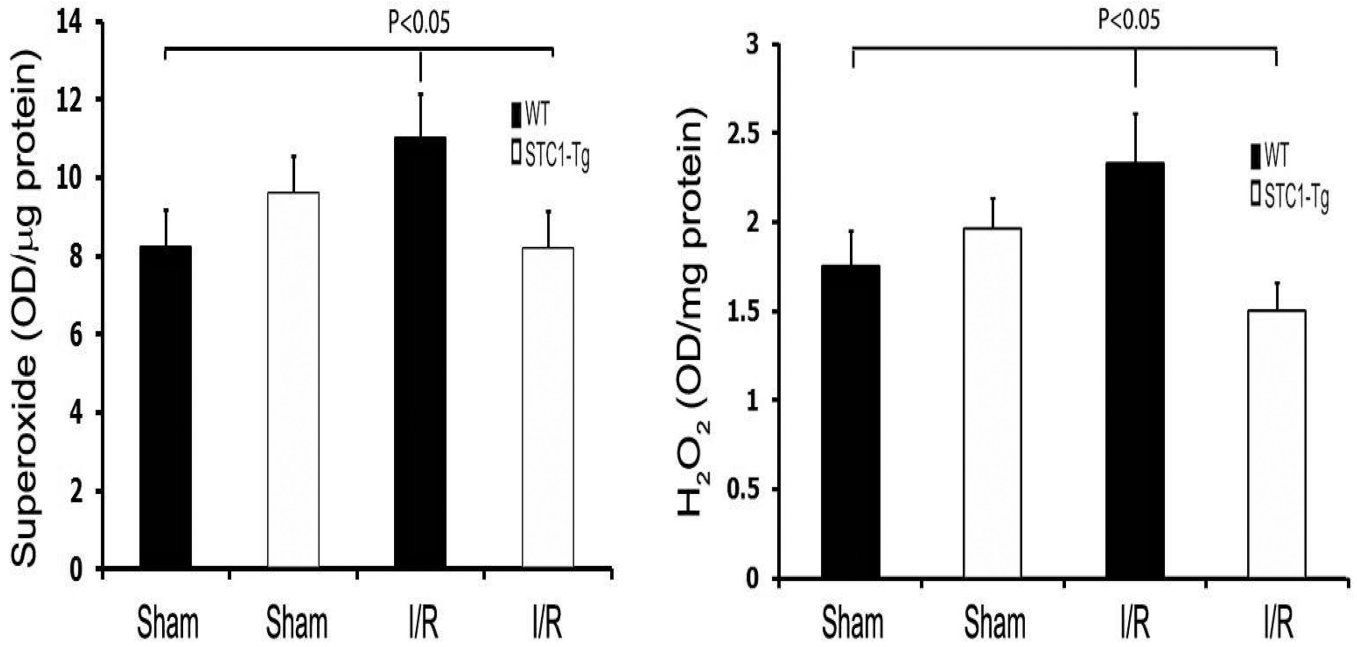

Figure 8. Increased generation of superoxide and H_2O_2 after I/R in WT kidneys, but not in STC1 Tg kidneys

Mice were killed 24h following I/R and kidneys were analyzed for superoxide and H_2O_2 using semi-quantitative methods. Bar graphs represent the means (± SEM) of data obtained from at least 6 mice from each group, and show marked elevation of both superoxide and H_2O_2 in WT kidneys after I/R, but not in STC1 Tg kidneys.

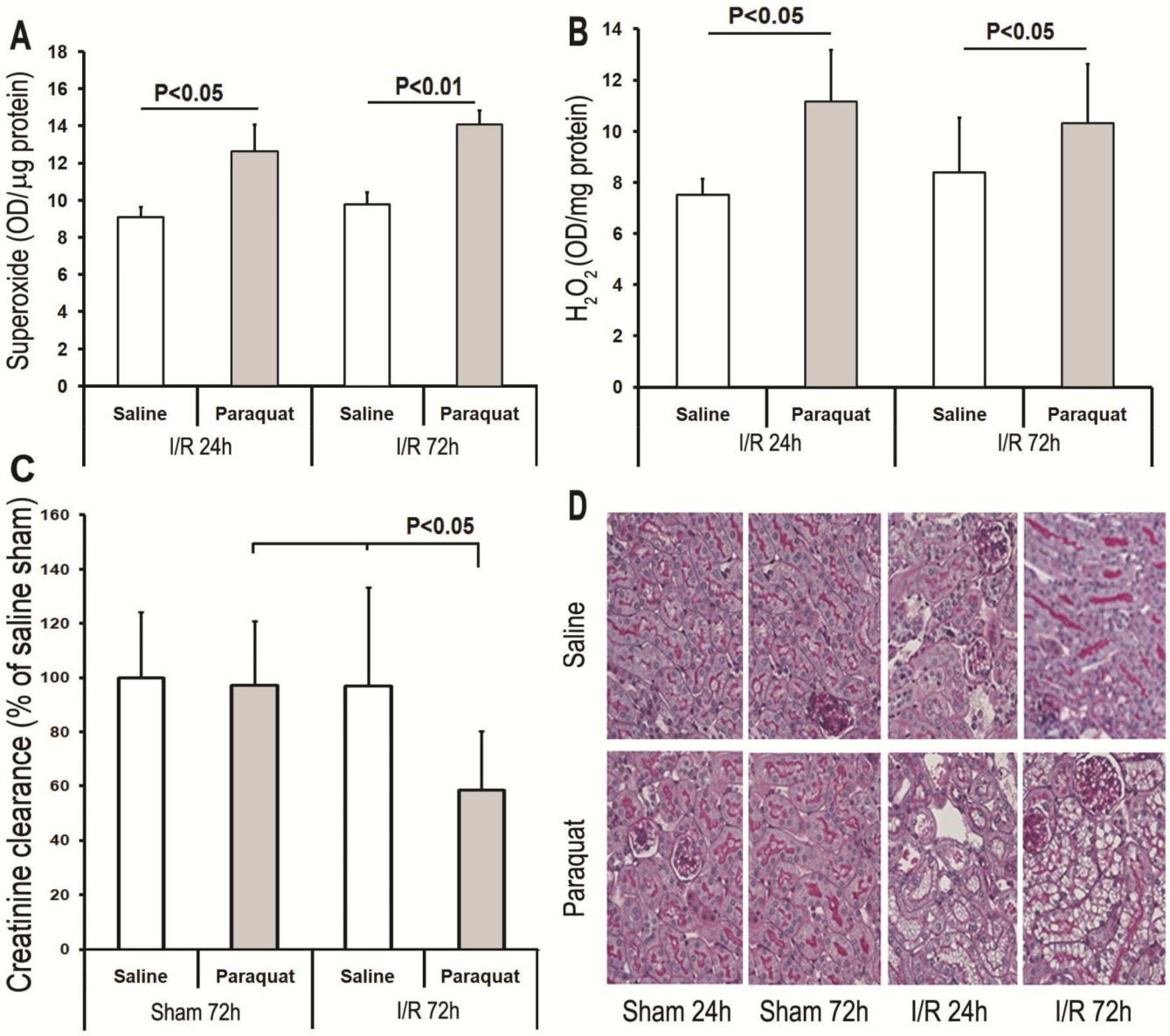

Figure 9. STC1 protects from I/R kidney injury through suppression of oxidant stress

STC1 Tg mice were given a single i.p. injection of saline or paraquat (12.5 mg/kg) 2h before clamping, and killed 24h, or 72h following I/R. Superoxide (**A**), H_2O_2 (**B**), CrCl expressed as % of saline-treated sham controls (**C**) and PAS staining for morphology (**D**) were carried out as detailed in methods. Bar graphs (**A, B and C**) represent data from at least 6 mice for each group/time point, and depict the mean values (± SEM). Representative PAS-stained images are shown in **D**. In paraquat-pretreated STC1 Tg mice, I/R results in: increased superoxide and H_2O_2 levels at the 24h through the 72h time points post I/R; drop in CrCl at the 72h post I/R, and morphological changes similar to those observed in WT mice after I/R. Representative images are shown (magnification 200X).

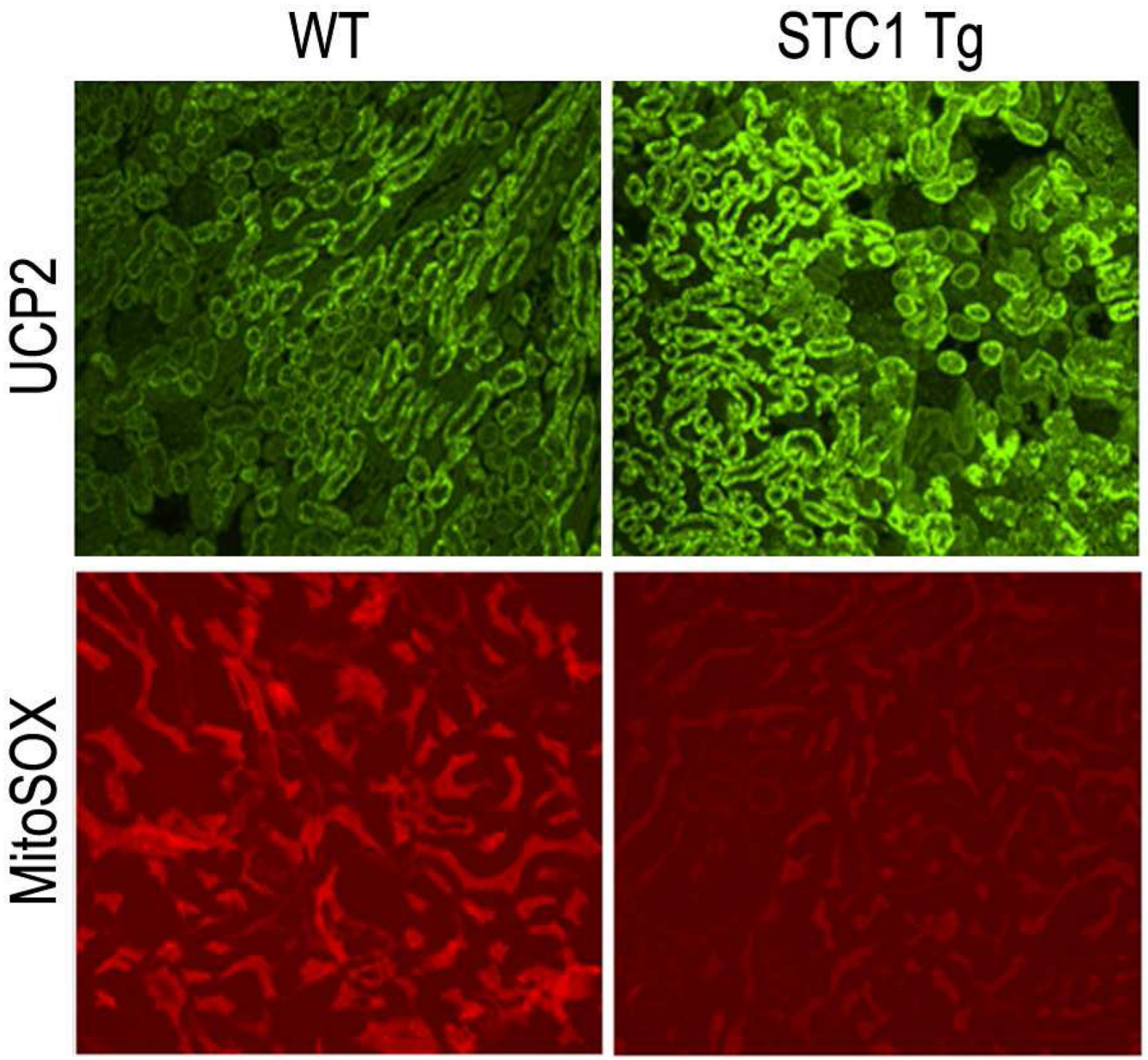

Figure 10. Increased expression of UCP2 in tubular epithelium of STC1 Tg kidneys correlates with decreased superoxide generation

Upper panels: Methacarn-fixed kidney sections from WT and STC1 Tg mice where stained with anti-UCP2, followed by FITC-labeled secondary antibodies. Representative images are shown (magnification 200X), and demonstrate higher level expression of UCP2 in tubular epithelial cells of STC1 Tg kidneys. Lower panels: freshly-isolated kidney slices were incubated with MitoSOX for 10 min, fixed in 4% paraformaldehyde and paraffin-imbedded; 5 μM sections were viewed under fluorescence microscope. Representative images are shown (magnification 200X), and demonstrate lower level MitoSOX red fluorescence (superoxide) in tubular epithelial cells of STC1 Tg kidneys, corresponding to higher levels of UCP2 expression.